Journal of Visualization, Vol. 11, No. 2 (2008)115-124

Regular Paper

Modification of Junction Flows by Altering the Section Shapes of the Cylinders

Wei, Q. D.*[1], Wang, J. M.*[1], Chen, G.*[2], Lu, Z. B.*[3] and Bi, W. T.*[4]

*1 State Key Laboratory of Turbulence and Complex System, College of Engineering, Peking University, Beijing 100871, China. E-mail: qdwei@pku.edu.cn
*2 Department of Computer Science, Johns Hopkins University, Baltimore, MD 21218, USA.
*3 The Institute of Applied Mathematics and Mechanics, Shanghai University, Shanghai, China.
*4 The Key Laboratory of Enhanced Heat Transfer and Energy Conservation, Ministry of Education of China, College of Environmental and Energy Engineering, Beijing University of Technology, Beijing, China.

Received 14 November 2007
Revised 12 February 2008

Abstract: Through visualization and measurement on the cylinder-plate junction flow, we show the horseshoe vortices can be significantly modified by altering the section shape of the cylinder. Both smoke-wire and Laser-Induced-Fluorescence (LIF) are employed to visualize the vortex structures. Laser Doppler velocimeter is used to measure the velocity field in the symmetry plane upstream of the cylinder. Electrical pressure-scanning valve is applied to acquire the pressure on the plate. It is found that, the sharper the frontal shape of the cylinder, the closer the vortex shedding position and the primary horseshoe vortex location to the cylinder. We quantitatively show the variation of the scale and strength of the primary horseshoe vortex, as well as the maximum wall shear stress, when the section shape of the cylinder is varied. The reduced streamwise adverse pressure gradient explains why the horseshoe vortices are significantly suppressed when the frontal shape of the cylinder becomes sharper. At last, we present a swept thin cylinder installed in front of the primary cylinder can be used to suppress the horseshoe vortices, which is greatly effective and easy to implement.

Keywords: Junction flow, Horseshoe vortex, Smoke wire, Laser induced fluorescence.

1. Introduction

Junction flow occurs when a boundary layer encounters an obstacle mounted on the same surface. Practically, there are a lot of obstacle-surfaces where junction flow exists, such as building-ground, pier-riverbed, wing-body, and sail-hull of a submarine, etc. Junction flow is characterized by three-dimensional boundary layer separation and horseshoe vortices that wrap around the obstacle. Both the wide application and the complex vortex dynamics have stimulated extensive studies on junction flow, as recently reviewed by Simpson R.L. (2001).

The presence of the horseshoe vortices has usually an unfavorable impact on the flow properties in the junction region. For example, the strong shear stresses due to the horseshoe vortices in a pier-riverbed junction increase erosion at the base of the pier and hence threaten the safe of the bridge. As another example, the horseshoe vortices in the sail-hull junction region of a submarine engender flow noise and structure vibration. In addition, the vortex legs may impinge upon and interfere with the propeller. Because of such problems, modification of the horseshoe vortex structures frequently becomes important in practice.

Scientists have tried many methods to restrict the horseshoe vortices. The vortices can be well suppressed by surface suction (e.g., Philips et al., 1992; Johnson et al., 1994; Seal and Smith, 1999) or boundary layer blowing (e.g., Johnson et al., 1994), which are two active control methods. Considering the energy efficiency and the practical feasibility, passive control methods are more attractive. Upstream ribbed surface is shown effective in modifying the turbulent junction vortex (e.g., Kairouz and Rahai, 2002; Nelson et al., 2003). In the junction region, some supplemental devices have been installed and displayed great performances, such as an inverted delta wing (e.g., Gupta, 1987) and a leading-edge fillet (e.g., Davenport et al., 1992; Barberis et al., 1998).

Because the adverse pressure gradient is the origin of the boundary layer separation and the horseshoe vortices in the junction region, a way to suppress the horseshoe vortices is to decrease the adverse pressure gradient, which can be done simply and fundamentally by reducing the frontal bluntness of the obstacle. The method is recognized (e.g., Metha, 1984), but quantitative and systematical studies are still lacking. Through visualization and measurement on a cylinder-flat-plate junction flow, the present study reveals how the variation of the section shape of the cylinder can significantly modify the horseshoe vortex structures in front of the cylinder. Besides, a promising new passive control method is introduced, which employs a swept thin cylinder to suppress the horseshoe vortices.

2. Experimental Apparatus

2.1 Wind Tunnel and Water Tunnel

We studied the cylinder-flat-plate junction flow by visualization and measurement. Smoke-wire visualization and pressure measurement were conducted in the Boundary Layer Wind Tunnel 1 of Peking University, China. The test section of the wind tunnel is 5.0 m long, 0.6 m wide and 0.6 m high. The free stream turbulence intensity is less than 0.2 %. LIF (Laser Induced Fluorescence) visualization and LDV (Laser Doppler Velocimeter) measurement were conducted in the Low Turbulence Water Tunnel of Peking University. The test section of the water tunnel is 6.0 m long, 0.4 m wide and 0.4 m high. The free stream turbulence intensity is less than 0.3 %.

2.2 Experimental Models

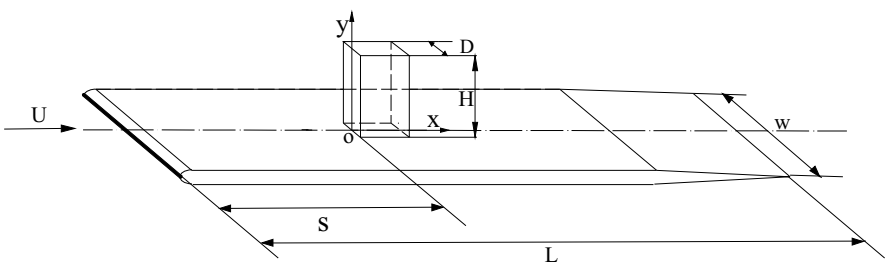

Fig. 1. The flat plate and cylinder.

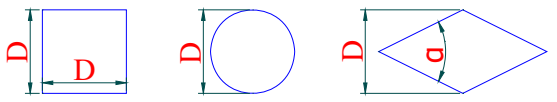

Fig. 2. The different section shapes of the cylinders.

The configuration of the experimental model is shown in Fig. 1. The flat plate, with an elliptic leading edge and a tapered trailing edge, has a length L and a width W. The cylinder is mounted on the centre-line of the plate and S away from the leading edge. The cylinder has a windward width D and a height H. For the smoke wire visualization and pressure measurement in the wind tunnel, L = 1,200 mm, W = 595 mm, S = 600 mm, D = 40 mm and H = 200 mm. For the LIF visualization and LDV measurement in the water tunnel, L = 2,000 mm, W = 395 mm, S = 700 mm, D = 80 mm and H = 160 mm. The height-to-diameter ratio H/D has an important effect in the behavior of horseshoe vortex systems (e.g., Rodriguez-y-Dominguez et al., 2006), and it is worth mentioning that at H/D > 1.5, the length of the separation region does not depend on H (e.g., Baker, 1980). Three kinds of cylinders are studied, which are respectively the square cylinder, the circular cylinder and the prism

(Fig. 2). For the prism, three interior angles are tested: α = 30°, 60° and 90°, respectively. The coordinate system O(X,Y) is shown in Fig. 1.

2.3 Experimental Facilities and Techniques

A smoke-wire device was used to visualize the junction flow in the wind tunnel. The smoky material was liquid paraffin. The wire was made of constantan and had a diameter of 50 μm. According to the visualization result, the wires were set to about 6 mm above the flat plate for the top view of the horseshoe vortex system.

LIF was used to visualize the junction vortices in the water tunnel. The laser source was a 5W Argon-ion laser. Green fluorescence dye was released very upstream to visualize the vortex shedding from the boundary layer, while red fluorescence dye was released near the junction to visualize the primary vortex as well as the inverse flow. The laser sheet was in the symmetry plane.

We used a TSI two-dimensional Laser-Doppler-Velocimeter (LDV) to measure the ensemble-averaged velocity field of the junction flow in the water tunnel. Although the Particle Image Velocimetry (PIV) is currently more popular, LDV is more appropriate than PIV in measuring flows with large velocity differences and strong shears, which are just the features of the junction flow. The velocities in the symmetry plane upstream of the cylinder were measured at unevenly-distributed rectangular grids to capture the vortex and resolve the near-plate shear.

The surface pressure on the flat plate was measured upstream of the cylinder along the half-width line of the plate in the wind tunnel. A HYSCAN2000 electrical pressure scanning valve (ZOC33 module) was used. Totally thirteen pressure holes were monitored. The sample frequency for each channel was 100 Hz and the sample time was 60 s. The precision of the scanning valve was 0.2 ‰. A restrictor connected to each pressure tube allowed a flat frequency response up to about 200 Hz.

3.Results

3.1 Visualization of the Laminar Junction Flows for Different Cylinders

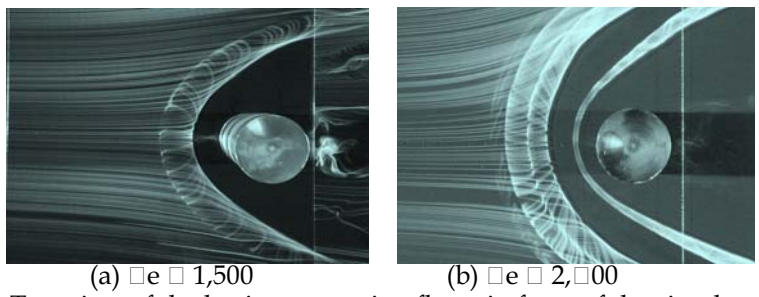

(a) □e □ 1,500 (b) □e □ 2,□00

Fig. □. Top □iew of the la□inar □unction flows in front of the circular cylinder.

Laminar junction flows occur at low Reynolds numbers. The Reynolds number is defined by Re = UD / υ, where U is the oncoming flow velocity. As the Reynolds number increases from a very small number, the laminar junction flow changes from a single primary horseshoe vortex (Fig. 3(a)) to multiple vortices (Fig. 3(b)) and the vortex system changes from steady state to periodic oscillation. When the Reynolds number continues to increase, the oscillation of the vortex system loses its periodicity. After that, small scale structures appear intermittently and the junction flow goes to turbulence (e.g., Khan, 1995; Wei et al., 2001).

The oscillating horseshoe vortex system can be well visualized by LIF from the side view. Figure 4 shows the horseshoe vortex systems in front of the three kinds of cylinders. The photos have been taken at approximately the same phase for a comparison. Affected by the streamwise adverse pressure gradient, the shear layer in the boundary layer rolls up into discrete vortices, as visualized by the green fluorescence in Fig. 4. The position where the vortex is shed downstream is similar for the square cylinder and the circular cylinder, while it is clearly postponed for the prism. The red fluorescence shows the primary horseshoe vortex. Comparing with the square and circular cylinders, the size of the primary horseshoe vortex of the prism is much smaller and the location is much closer to the cylinder.

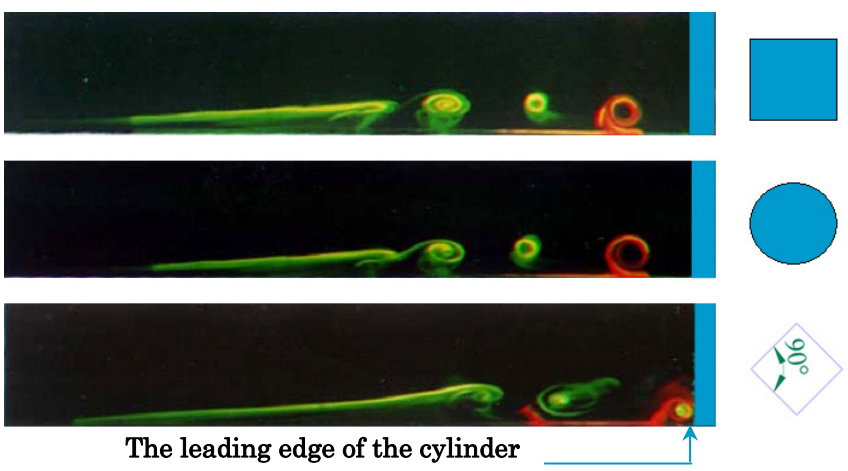

Fig. 4. Side □iew of the la□inar □unction flows ahead of different cylinders at □e □ 4,000

Top view of the oscillating laminar junction flows in front of the different cylinders is shown in Fig. 5. Although we cannot capture the images at precisely the same phase during the oscillation of the horseshoe vortex systems, we clearly see from the top view that the vortex systems get closer to the cylinder when the cylinder section shape changes from square to rhombus with 60° interior angle (Figs. 5(a)-(d)). Especially, the location of the primary horseshoe vortex in the prism junction flow is very close to the prism, which is consistent with the side-view visualization by LIF.

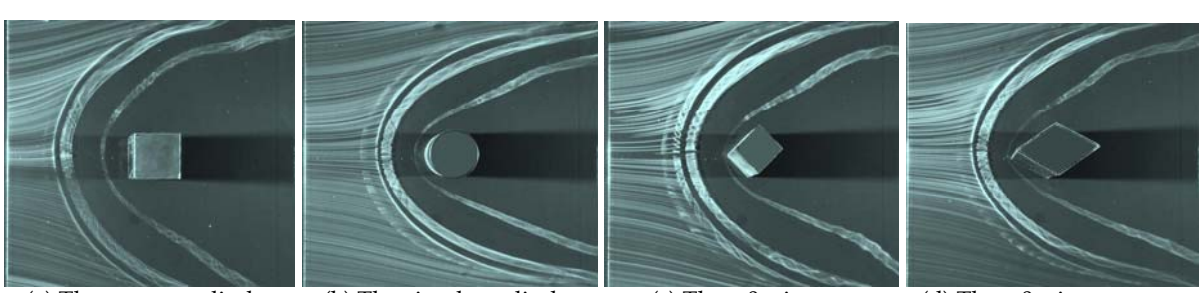

(a) The s□uare cylinder (b) The circular cylinder (c) The □0p̄ris□ (d) The □0p̄ris□

Fig. 5. Top □iew of the la□inar □unction flows ahead of different cylinders at □e □ 4,000.

To conclude, through the smoke and LIF flow visualization, we show that when the frontal shape of an obstacle becomes sharper, the vortex shedding position, the location of the primary horseshoe vortex, as well as the separation line on the flat plate, get close to the obstacle, and the dimension of the primary vortex is reduced.

3.2 The Velocity Fields of the Turbulent Junction Flows for Different Cylinders

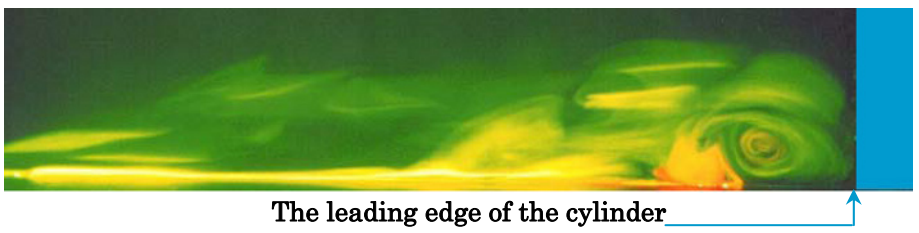

Fig. □. Side □iew of the turbulent □unction flow ahead of the s□uare cylinder at □e □ □2,000.

Most of practical junction flows are fully turbulent. Unlike the oscillating laminar junction flow, the turbulent junction flow has a primary horseshoe vortex that varies only slightly in terms of location, size and circulation (Fig. 6). We have measured the ensemble-averaged velocity fields in the upstream symmetry plane of the turbulent junction flows using LDV. As an example, Fig. 7 shows the average velocity distribution in the junction region of the square cylinder at Re = 32,000.

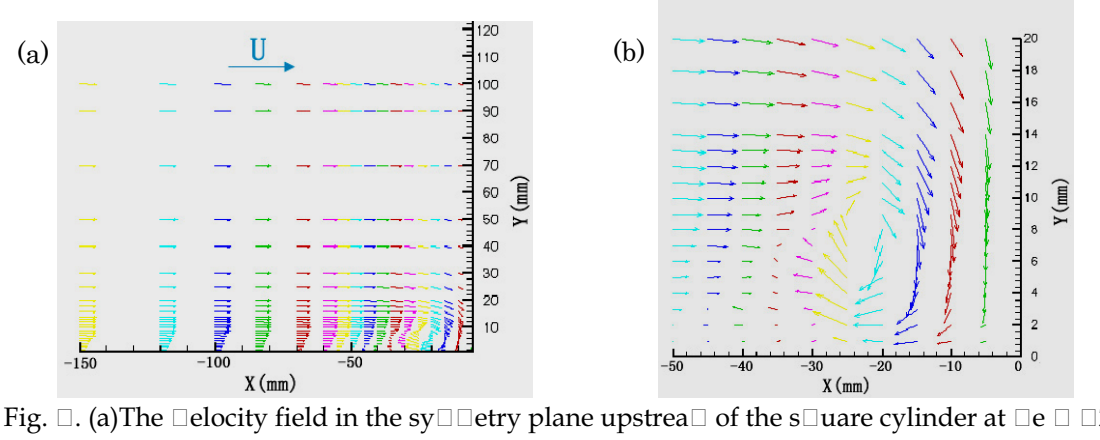

Fig. □. (a)The □elocity field in the sy□□etry plane upstrea□ of the s□uare cylinder at □e □ □2,000□ (b) zoo□ in of (a) around the pri□ary □uncture □orte□.

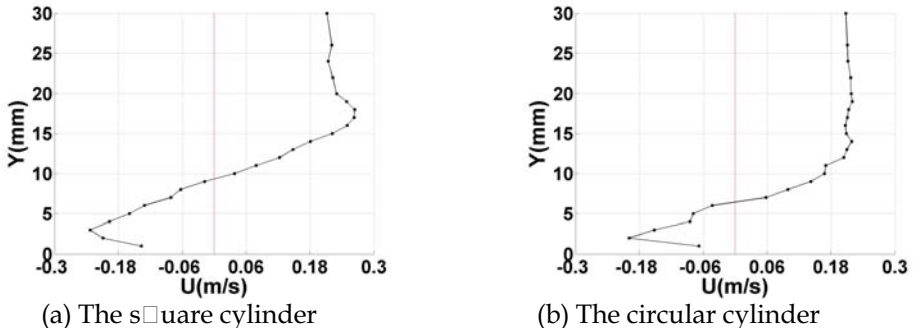

(a) The s□uare cylinder (b) The circular cylinder

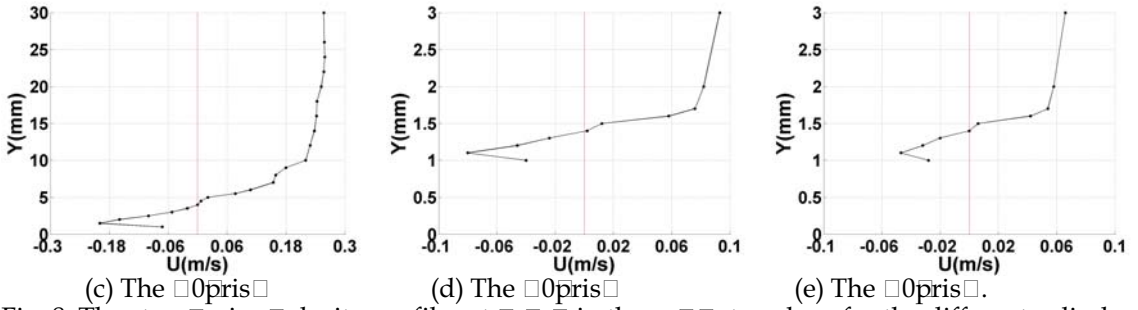

(c) The □0□pris□ (d) The □0□pris□ (e) The □0□pris□.

Fig. 8. The strea□wise □elocity profiles at □ □ □ in the sy□□etry plane for the different cylinders. (□,□) is the center of the pri□ary horseshoe □orte□ (□e □ □2,000).

We use the Rankine vortex to model the primary horseshoe vortices as displayed in Fig. 7(b). In the core of the Rankine vortex, the velocity distribution is:

$$U_\theta(r) = \frac{U_m r}{L_v}$$

where U_m is the maximum velocity, L_v is the radius of the vortex core, $r = \sqrt{(x-X)^2 + (y-Y)^2}$ and (X,Y) is vortex center (e.g., Wu et al, 2005). We estimate U_m, L_v and (X,Y) by fitting the measured velocities with the Rankine vortex. For example, the vortex center in Fig. 7 is estimated (X,Y) = (-23.51 mm, 9.47 mm). The maximum velocity is U_m = 0.25 ms^{-1}, and the vortex radius is L_v = 6.23 mm. We define the strength of the primary horseshoe vortex by:

$$S = 2\pi U_m L_v$$

So the strength of the vortex in Fig. 7 is S = 0.0098 m^{2}s^{-1}. To be more visible, we plot the profile of the streamwise velocity component at x = X, which is computed by interpolation. The near linearity of the streamwise velocity profiles in Fig. 8 verifies our proposal of the Rankine-vortex-approximation. Because we have measured the flow velocities at only 1 mm above the flat plate (Fig. 8), we can estimate, albeit rather roughly, the maximum wall shear stress τ by:

$$\tau = \mu \frac{|U_{0.001}|}{0.001}$$

where μ is the kinematic viscosity of water and $U_{0.001}$ is the streamwise velocity at y = 1 mm in Fig. 8. The maximum wall shear stress in Fig.7 is 1.36×10^{-6} Pa. The characteristic quantities of the primary horseshoe vortices of the other cylinders are estimated relative to the corresponding data of the square cylinder, and given in Table 1.

The quantitative results in Table 1 extend the findings by flow visualization on the laminar junction flows. We find out that when the frontal bluntness is reduced from the square cylinder to the 30º prism, the center location of the primary horseshoe vortex moves significantly to the very vicinity of the cylinder-plate joint. The vortex radius of the prism is decreased to as small as one twentieth of that of the square cylinder. The vortex strength and the maximum wall shear stress of the 30º prism are, respectively, only 1 % and 20 % of those of the square cylinder.

Table 1. The characteristic □uantities of the pri□ary horseshoe □ortices for different cylinders at □e □ □2,000.

		Square cylinder	Circular cylinder	Prism (interior angle α)		
				α = 90º	α = 60º	α = 30º
Relative vortex center location	X	1.000	0.727	0.430	0.088	0.048
	Y	1.000	0.678	0.448	0.149	0.148
Relative vortex radius (Lv)		1.000	0.756	0.600	0.048	0.048
Relative vortex strength (S)		1.000	0.686	0.546	0.017	0.010
Relative maximum wall shear stress (τ)		1.0000	0.4926	0.5221	0.2868	0.2059

In conclusion, the frontal bluntness of an obstacle has a very important influence on the horseshoe vortex structures in the turbulent junction flow. If practically possible, altering the section shape of an obstacle, from square to rhombus for example, benefits a lot by a much smaller and weaker primary horseshoe vortex in front of the obstacle.

3.3 The Pressure Distributions of the Turbulent Junction Flows for Different Cylinders

The streamwise adverse pressure gradient is recognized as the origin of the three dimensional separation in the junction flow. By measuring the pressure distribution on the upstream flat plate, we can evaluate the influence of the different cylinders on the horseshoe vortex systems. In Fig. 9, we show the mean and root-mean-square surface pressure coefficients measured in the upstream symmetry plane for the three kinds of cylinders. From Figs. 9(a), (c) and (e), the mean surface pressure coefficients immediately ahead of the cylinder-plate joints are 0.9~1.0 for the square cylinder, 0.8~0.85 for the circular cylinder and about 0.4 for the prism with 60° interior angle. On the whole, the adverse pressure gradient is significantly reduced relatively by the rhombus section shape of the prism, and the adverse pressure region in front of the circular cylinder is shorter than that in front of the square cylinder.

The V-structure in the mean surface pressure distribution of Fig. 9(a) displays the location and strength of the primary horseshoe vortex in front of the square cylinder (e.g., Baker, 1979 and 1980). The primary vortex entrains higher-speed free-stream fluid to the flat plate and causes the local surface pressure drop. The V-structure shows up in the circular cylinder junction flow (Fig. 9(c)), but it moves towards the cylinder and has a smaller magnitude. In front of the prism, there is not an apparent V-structure. The inverse-V-structures in the rms pressure distributions of Figs. 9(b) and (d) display the strong surface pressure fluctuations generated by the primary horseshoe vortices in front of the square and circular cylinders. The inverse-V-structure does not appear in front of the prism, revealing that the primary horseshoe vortex of the prism is much quiet.

From the V-structures and the inverse-V-structures in Fig. 9, we recover the result obtained by the flow visualization and the velocity measurement. That is, when the cylinder section shape

changes from square to circle and rhombus, the location of the primary horseshoe vortex gets closer to the cylinder and the strength reduces. The variation is along with the decrease of the streamwise adverse pressure gradient.

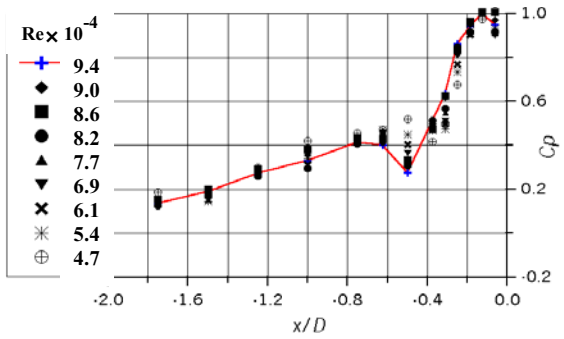

(a) Mean pressure coefficients ahead of the s□uare cylinder

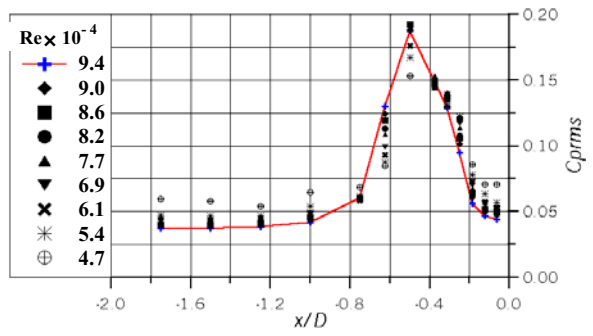

(b) r□s pressure coefficients ahead of the s□uare cylinder

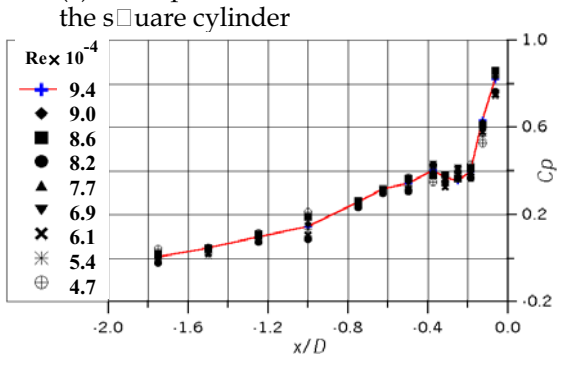

(c) Mean pressure coefficients ahead of the circular cylinder

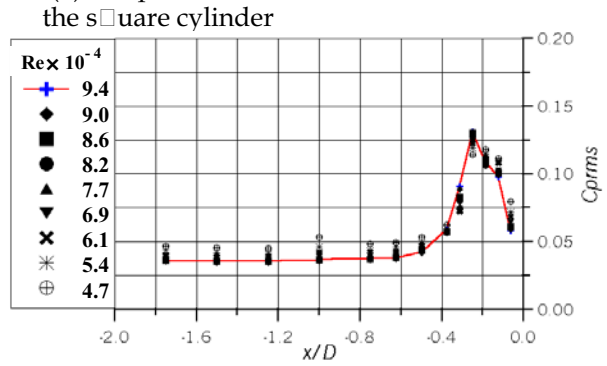

(d) r□s pressure coefficients ahead of the circular cylinder

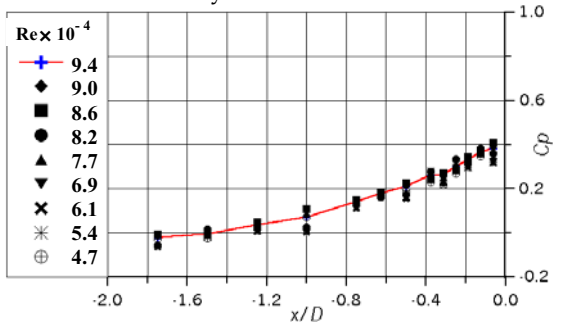

(e) Mean pressure coefficients ahead of the □0□pris□

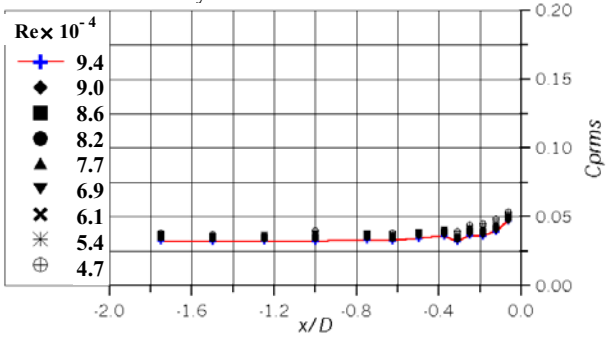

(f) r□s pressure coefficients ahead of the □0□pris□

Fig. □. The □ean and root □ean s□uare (r□s) surface pressure coefficients in the upstrea□ sy□□etry plane □easured for different cylinders at different □eynolds nu□bers.

3.4 Influence of a Swept Thin Circular Cylinder on the Junction Flows

Altering the frontal shape of an obstacle is sometimes not practically applicable. Enlightened by the passive control devices developed in the former studies (e.g., Gupta, 1987; Devenport et al., 1992; Barberis et al., 1998; Shao et al., 2007), we proposed a new method.

We installed a thin circular cylinder in front of the primary cylinder, with its top tip connecting with the primary cylinder at a height and its bottom tip connecting with the flat plate. The circular cylinder was selected as the thin swept cylinder because of its property of axis-symmetry that is not sensitive to wind direction. Therefore, the thin circular cylinder is sweptback (Fig. 10). For this experiment, the top tip of the swept thin circular cylinder connects with the square cylinder at a fixed height of 2.5D above the flat plate. The swept angle $\Phi = 0°$ corresponds to the situation when the thin circular cylinder is perpendicular to the flat plate.

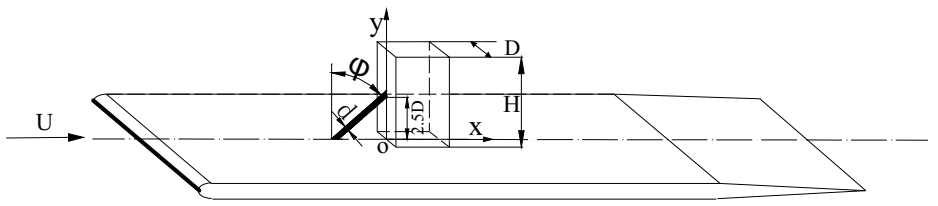

Fig. 10. The cylinder with a swept thin circular cylinder □ounted on it.

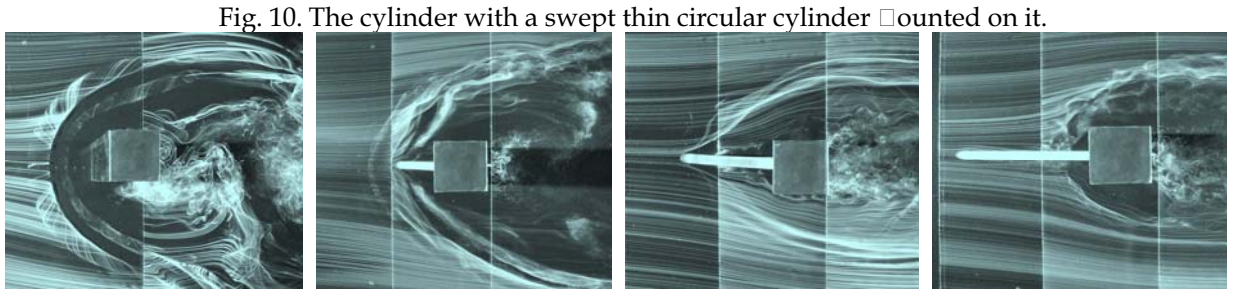

(a) The baseline □unction flow (b) 20□swept cylinder (c) 40□swept cylinder (d) 50□swept cylinder

Fig. 11. Modification of the horseshoe □orte□ syste□ using a swept thin circular cylinder at □e □ 5,□00. d□D □ 1□5.

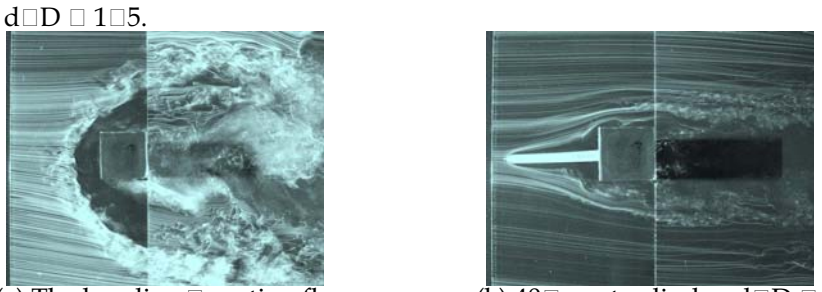

(a) The baseline □unction flow (b) 40□swept cylinder, d□D □ 1□5

Fig. 12. Modification of the horseshoe □orte□ syste□ using a 40□swept circular cylinder at □e □ 8,000.

In Fig. 11, we show the effect of the swept thin circular cylinder on the oscillating laminar junction flow. With a swept cylinder installed, the horseshoe vortex system is modified (Figs. 11(b), (c) and (d)). The uncontrolled flow is also visualized as the baseline flow (Fig. 11(a)). When the thin circular cylinder is installed at an appropriate swept angle, 40° for example (Fig. 11(c)), the horseshoe vortices can be eliminated and the wake becomes narrow. Figure 12 gives the case of nearly turbulent junction flow. The primary horseshoe vortex can also be eliminated by the swept thin circular cylinder. The swept cylinder also generates horseshoe vortices in front of it (see Fig. 11(c)). But because the cylinder is sweptback and the diameter is smaller, the horseshoe vortices are much weaker than those of the baseline flow (e.g., Zhang and Lv, 2000; Khan and Ahmed, 2001 and 2002).

We anticipate the streamwise adverse pressure gradient is reduced by the presence of the swept thin cylinder. It is indeed true. Figure 13 shows the mean and root mean square surface pressure coefficients measured in front of the circular cylinder at Re = 26,700, with and without control by the swept thin circular cylinder. The streamwise adverse pressure gradient is greatly reduced, except in the upstream vicinity of the joint between the swept cylinder and the flat plate, where the adverse pressure gradient is strengthened by the swept-cylinder-plate junction (Fig. 13(a)). On the other hand, the presence of the swept thin cylinder enhances the surface pressure fluctuations downstream of it (Fig. 13(b)). Nevertheless, the increased intensity of the pressure fluctuations is still much lower than the intensity of the pressure fluctuations generated by the primary horseshoe vortex in the baseline flow.

If seen as an extension of the nose of an obstacle, the swept thin cylinder reduces the frontal bluntness of the obstacle. As a result, it decreases the streamwise adverse pressure gradient and hence suppresses the horseshoe vortices in front of the obstacle. In this sense, the method is likely universal. The great performance, the easiness to implement and the probable universality make the swept thin cylinder a promising new method to control the horseshoe vortices in junction flows.

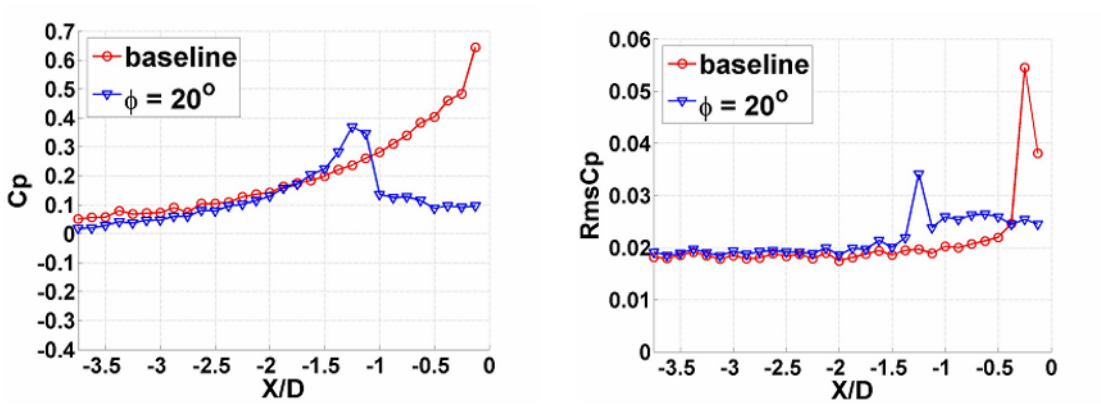

(a) Mean pressure coefficients (b) r□s pressure coefficients

Fig. 1□. The □ean and root □ean s□uare surface pressure coefficients □easured in the upstrea□ sy□□etry plane of the circular cylinder □unction flow at □e □ 2□,□00.

4. Conclusions

We experimentally studied the cylinder-plate junction flows to investigate the effects of the cylinder section shape on the horseshoe vortices. Flow visualization by smoke wire and Laser Induced Fluorescence on the laminar junction flows show that when the cylinder section shape changes from square to circle and rhombus, the location of the primary horseshoe vortex gets close to the cylinder and the size of the primary horseshoe vortex decreases. Quantitative measurements on the velocity field in the symmetry plane of the turbulent junction flows support the results of the flow visualization. In addition, the strength of the primary horseshoe vortex, as well as the maximum wall shear stress, is found significantly weakened by the prism in comparison with the square cylinder. Pressure measurements verify the above results and show the correlation between reduction of the streamwise adverse pressure gradient and suppression of the horseshoe vortices. The above findings highlight the significant influence of the frontal bluntness on the horseshoe vortex structures in the junction flows. Reducing the frontal bluntness, if practically possible, benefits a lot by a much smaller and weaker primary horseshoe vortex.

In the end, we proposed a new method to modify the horseshoe vortices in junction flows. A swept thin circular cylinder is installed in front of the primary cylinder. When it is put at an appropriate position, the horseshoe vortices can be eliminated and the wake narrows. Pressure measurements reveal that the streamwise adverse pressure gradient is reduced in the region between the swept cylinder and the primary cylinder.

Acknowledgement

The authors would like to thank Mr. Wang Y.L. of the State Key Laboratory of Turbulence and Complex System of Peking University for his kind help in the experiment.

References

Baker, C. J., The Laminar Horseshoe Vortex, J. Fluid Mech., 95 (1979), 347-367.

Baker, C. J., The Turbulent Horseshoe Vortex, Journal of Wind Engineering and Industrial Aerodynamics, 6(1980), 9-23.

Barberis, D., Molton, P. and Malaterre, T., Control of 3D Turbulent Boundary Layer Separation Caused by a Wing-body Junction, Experimental Thermal and Fluid Science, 16 (1998), 54-63.

Devenport, W. J., Simpson, R. L., Dewitz, M. B. and Agarwal, N. K., Effects of a Leading-Edge Fillet on the Flow Past an Appendage-Body Junction, AIAA Journal, 30-9 (1992).

Gupta, A. K., Hydrodynamic Modification of the Horseshoe Vortex at a Vertical Pier Junction with Ground, Phys. Fluids, 30-4 (1987).

Johnson, M.J., Ravindra K. and Andres R., Comparative Study of the Elimination of the Wing Fuselage Junction Vortex by Boundary Layer Suction And Blowing, AIAA-94-0293, (1994).

Kairouz, K. and Rahai, H. R., Turbulent Junction Vortex with Upstream Ribbed Surface, 20th AIAA Applied Aerodynamics Conference (St.Louis, Missouri), AIAA-2002-3262, (2002-6).

Khan, M. J., Ahmed, A. and Trosper, J. R., Dynamics of the Juncture Vortex, AIAA Journal, 33-7 (1995).

Khan, M. J. and Ahmed, A., Vorticity and its Transport in Juncture Flow, 19th Applied Aerodynamics Conference AIAA-2001-2479, (2001-6).

Khan, M. J. and Ahmed, A., On the Juncture Vortex in the Transverse Planes, 40th AIAA Aerospace Sciences Meeting&Exhibit (Reno, NV), AIAA-2002-0163, (2002-1).

Metha, R. D., Effect of Wing Nose Shape on the Flow in a Wing-Body Junction, Aeronautical Journal, 88 (1984), 40-48.
Nelson, R., Elizarraras, G, and Rahai, H. R., Effects of an upstream Ribbed Surface on the Flow Past a Cylinder-Flat Plate Junction, 41st Aerospace Sciences Meeting and Exhibit (Nevada), AIAA-2003-428, (2003-1).
Philips, D. B., Cimbala, J. M. and Treaster, A. L., Suppression of the Wing-Body Junction Vortex by Body Surface Suction, J. Aircraft, 29 (1992), 118-122.
Rodriguez y Dominguez, M., Romero-Mendez, R., Ramos-Palau, M. and Perez-Gutierrez, F. G., The Laminar Horseshoe Vortex Upstream of a Short-Cylinder Confined in a Channel Formed by a Pair of Parallel Plates, Journal of Visualization, 9-3 (2006), 309-318.
Seal, C. V. and Smith, C. R., The Control of Turbulent End-Wall Boundary Layers Using Surface Suction, Experiments in Fluids, 27 (1999), 484-496.
Shao, C. P., Wang, J. M. and Wei, Q. D., Visualization Study on Suppression of Vortex Shedding from a Cylinder, Journal of Visualization, 10-1 (2007), 57-64.
Simpson, R. L., Junction Flows, Annu Rev. Fluid Mech., 33 (2001), 415-43.
Wei, Q. D., Chen, G. and Du, X. D., An Experimental Study on the Structure of Juncture Flows, Journal of Visualization, 3-4 (2001).
Wu, J. Z., Ma, H. Y. and Zhou, M. D., Vorticity and Vortex Dynamics, (2005-8), 260, Springer-Verlag,.
Zhang, H. and Lv Z. Y., Experimental investigation of vortex characteristics in swept wing/body junctions, Experiments and Measurements in Fluid Mechanics, 14-2 (2000).

Author Profile

Qing-Ding Wei: He graduated in the Department of Mathematics and Mechanics from Peking University in 1963. He worked in 7th Institute of Aerodynamic Academy of China as a researcher from 1968 to 1976, and then he worked at Peking University up to now. He received his Ph. D degree in 1981 from the University of Tokyo. Now he works at State Key Laboratory of Turbulence and Complex System (Peking University) as a professor. His research interests are environmental fluid dynamics, experimental fluid mechanics and wind engineering.

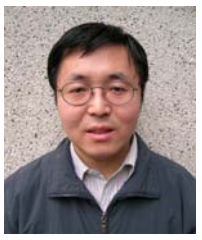

Jian-Ming Wang: He is pursuing a PhD in Peking University.

Guang Chen: He received his Master's Degree in Mechanics in1999 from the Department of Mechanics and Engineering Science of Peking University. He is currently pursuing a PhD in Johns Hopkins University.

Zhan-Bin Lu: He received his Master's Degree in Fluid Mechanics from Peking University (China) in 2000, and PhD in Mechanical Engineering from Northwestern University (USA) in 2003. Currently, he is an assistant professor at the Institute of Applied Mathematics and Mechanics, Shanghai University. His research interests are computational fluid dynamics and combustion.

Wei-Tao Bi: He obtained his PhD degree from the Department of Mechanics and Engineering Science of Peking University in 2002. After that, he went to the University of Tokyo and then Universite de Rennes 1 as a postdoc. Now he works as a research scientist at the College of Environmental and Energy Engineering of Beijing University of Technology. His research interests include experimental fluid mechanics, heat and mass transfer, and physics of granular media.